Dynamic mechanical characterization with respect to temperature, humidity, frequency and strain in mPOFs made of different materials

Leal-Junior, A.; Frizera, A.; Pontes, M. J.; Fasano, Andrea; Woyessa, Getinet; Bang, Ole; Marques, C. A.F.

Published in:
Optical Materials Express

Link to article, DOI:
10.1364/OME.8.000804

Publication date:
2018

Document Version
Publisher's PDF, also known as Version of record

Research Article | Vol. 8, No. 4 | 1 Apr 2018 | OPTICAL MATERIALS EXPRESS 804
Optical Materials EXPRESS

Dynamic mechanical characterization with respect to temperature, humidity, frequency and strain in mPOFs made of different materials

A. LEAL-JUNIOR,[1,*] A. FRIZERA,[1] M. J. PONTES,[1] A. FASANO,[2] G. WOYESSA,[3] O. BANG,[3,4] AND C. A. F. MARQUES[5]

[1]*Graduate Program of Electrical Engineering of Federal University of Espirito Santo, Vitória, Brazil*
[2]*DTU Mekanik, Department of Mechanical Engineering, Technical University of Denmark, Denmark*
[3]*DTU Fotonik, Department of Photonics Engineering, Technical University of Denmark, Denmark*
[4]*SHUTE Sensing Solutions APS, Diplomvej 381, 2800 Kongens Lyngby, Denmark*
[5]*Instituto de Telecomunicações and Physics Department & I3N, Universidade de Aveiro, Campus Universitário de Santiago, 3810-193 Aveiro, Portugal*
**arnaldo.leal@aluno.ufes.br*

Abstract: This paper presents a dynamic mechanical analysis (DMA) of polymer optical fibers (POFs) to obtain their Young modulus with respect to the variation of strain, temperature, humidity and frequency. The POFs tested are made of polymethyl methacrylate (PMMA), Topas grade 5013, Zeonex 480R and Polycarbonate (PC). In addition, a step index POF with a core composed of Topas 5013 and cladding of Zeonex 480R is also analyzed. Results show a tradeoff between the different fibers for different applications, where the Zeonex fiber shows the lowest Young modulus among the ones tested, which makes it suitable for high-sensitivity strain sensing applications. In addition, the fibers with Topas in their composition presented low temperature and humidity sensitivity, whereas PMMA fibers presented the highest Young modulus variation with different frequencies. The results presented here provide guidelines for the POF material choice for different applications and can pave the way for applications involving the combination of different polymer materials.

OCIS codes: (160.5470) Polymers; (160.4670) Optical materials; (220.0220) Optical design and fabrication; (280.4788) Optical sensing and sensors.

References and links

1. D. J. Webb, "Fibre Bragg grating sensors in polymer optical fibres," Meas. Sci. Technol. **26**(9), 092004 (2015).
2. C. Markos, J. C. Travers, A. Abdolvand, B. J. Eggleton, and O. Bang, "Hybrid photonic-crystal fiber," Rev. Mod. Phys. **89**(4), 045003 (2017).
3. Y. Koike and M. Asai, "The future of plastic optical fiber," NPG Asia Mater. **1**(1), 22–28 (2009).
4. K. Peters, "Polymer optical fiber sensors—a review," Smart Mater. Struct. **20**(1), 013002 (2011).
5. K. Makino, T. Kado, A. Inoue, and Y. Koike, "Low loss graded index polymer optical fiber with high stability under damp heat conditions," Opt. Express **20**(12), 12893–12898 (2012).
6. W. Zhang, D. J. Webb, and G.-D. Peng, "Enhancing the sensitivity of poly(methyl methacrylate) based optical fiber Bragg grating temperature sensors," Opt. Lett. **40**(17), 4046–4049 (2015).
7. G. Woyessa, K. Nielsen, A. Stefani, C. Markos, and O. Bang, "Temperature insensitive hysteresis free highly sensitive polymer optical fiber Bragg grating humidity sensor," Opt. Express **24**(2), 1206–1213 (2016).
8. A. Fasano, G. Woyessa, P. Stajanca, C. Markos, A. Stefani, K. Nielsen, H. K. Rasmussen, K. Krebber, and O. Bang, "Fabrication and characterization of polycarbonate microstructured polymer optical fibers for high-temperature-resistant fiber Bragg grating strain sensors," Opt. Mater. Express **6**(2), 649 (2016).
9. A. R. Prado, A. G. Leal-Junior, C. Marques, S. Leite, G. L. de Sena, L. C. Machado, A. Frizera, M. R. N. Ribeiro, and M. J. Pontes, "Polymethyl methacrylate (PMMA) recycling for the production of optical fiber sensor systems," Opt. Express **25**(24), 30051–30060 (2017).
10. C. A. F. Marques, G.-D. Peng, and D. J. Webb, "Highly sensitive liquid level monitoring system utilizing polymer fiber Bragg gratings," Opt. Express **23**(5), 6058–6072 (2015).
11. A. Stefani, S. Andresen, W. Yuan, N. Herholdt-Rasmussen, and O. Bang, "High sensitivity polymer optical fiber-bragg-grating-based accelerometer," IEEE Photonics Technol. Lett. **24**(9), 763–765 (2012).
12. H. U. Hassan, J. Janting, S. Aasmul, and O. Bang, "Polymer Optical Fiber Compound Parabolic Concentrator

#322620 https://doi.org/10.1364/OME.8.000804
Journal © 2018 Received 5 Feb 2018; revised 17 Feb 2018; accepted 27 Feb 2018; published 7 Mar 2018

Optical Materials EXPRESS

fiber tip based glucose sensor: in-Vitro Testing," IEEE Sens. J. **16**, 8483–8488 (2016).
13. N. Zhong, M. Zhao, L. Zhong, Q. Liao, X. Zhu, B. Luo, and Y. Li, "A high-sensitivity fiber-optic evanescent wave sensor with a three-layer structure composed of Canada balsam doped with GeO2," Biosens. Bioelectron. **85**, 876–882 (2016).
14. J. Jensen, P. Hoiby, G. Emiliyanov, O. Bang, L. Pedersen, and A. Bjarklev, "Selective detection of antibodies in microstructured polymer optical fibers," Opt. Express **13**(15), 5883–5889 (2005).
15. C. A. F. Marques, D. J. Webb, and P. Andre, "Polymer optical fiber sensors in human life safety," Opt. Fiber Technol. **36**, 144–154 (2017).
16. G. Rajan, Y. M. Noor, B. Liu, E. Ambikairaja, D. J. Webb, and G. D. Peng, "A fast response intrinsic humidity sensor based on an etched singlemode polymer fiber Bragg grating," Sens. Actuators A Phys. **203**, 107–111 (2013).
17. W. Zhang and D. J. Webb, "PMMA Based Optical Fiber Bragg Grating for Measuring Moisture in Transformer Oil," IEEE Photonics Technol. Lett. **28**(21), 2427–2430 (2016).
18. W. Yuan, A. Stefani, and O. Bang, "Tunable polymer fiber Bragg grating (FBG) inscription: Fabrication of dual-FBG temperature compensated polymer optical fiber strain sensors," IEEE Photonics Technol. Lett. **24**(5), 401–403 (2012).
19. W. Yuan, L. Khan, D. J. Webb, K. Kalli, H. K. Rasmussen, A. Stefani, and O. Bang, "Humidity insensitive TOPAS polymer fiber Bragg grating sensor," Opt. Express **19**(20), 19731–19739 (2011).
20. G. Woyessa, A. Fasano, C. Markos, A. Stefani, H. K. Rasmussen, and O. Bang, "Zeonex microstructured polymer optical fiber: fabrication friendly fibers for high temperature and humidity insensitive Bragg grating sensing," Opt. Mater. Express **7**(1), 286 (2017).
21. C. Markos, A. Stefani, K. Nielsen, H. K. Rasmussen, W. Yuan, and O. Bang, "High-Tg TOPAS microstructured polymer optical fiber for fiber Bragg grating strain sensing at 110 degrees," Opt. Express **21**(4), 4758–4765 (2013).
22. K. Nielsen, H. K. Rasmussen, A. J. Adam, P. C. Planken, O. Bang, and P. U. Jepsen, "Bendable, low-loss Topas fibers for the terahertz frequency range," Opt. Express **17**(10), 8592–8601 (2009).
23. M. C. J. Large, J. Moran, and L. Ye, "The role of viscoelastic properties in strain testing using microstructured polymer optical fibres (mPOF)," Meas. Sci. Technol. **20**(3), 034014 (2009).
24. O. Ziemann, J. Krauser, P. E. Zamzow, and W. Daum, *POF Handbook: Optical Short Range Transmission Systems* (2008).
25. R. Oliveira, L. Bilro, and R. Nogueira, "Bragg gratings in a few mode microstructured polymer optical fiber in less than 30 seconds," Opt. Express **23**(8), 10181–10187 (2015).
26. M. G. Kuzyk, U. C. Paek, and C. W. Dirk, "Guest-Host Fibers for Nonlinear Optics," Appl. Phys. Lett. **59**(8), 902–904 (1991).
27. J. Zubia and J. Arrue, "Plastic Optical Fibers: An Introduction to Their Technological Processes and Applications," Opt. Fiber Technol. **7**(2), 101–140 (2001).
28. G. Woyessa, A. Fasano, A. Stefani, C. Markos, K. Nielsen, H. K. Rasmussen, and O. Bang, "Single mode step-index polymer optical fiber for humidity insensitive high temperature fiber Bragg grating sensors," Opt. Express **24**(2), 1253–1260 (2016).
29. A. Stefani, S. Andresen, W. Yuan, and O. Bang, "Dynamic characterization of polymer optical fibers," IEEE Sens. J. **12**(10), 3047–3053 (2012).
30. A. G. L. Junior, A. Frizera, and M. J. Pontes, "Analytical model for a polymer optical fiber under dynamic bending," Opt. Laser Technol. **93**, 92–98 (2017).
31. I.-L. Bundalo, K. Nielsen, G. Woyessa, and O. Bang, "Long-term strain response of polymer optical fiber FBG sensors," Opt. Mater. Express **7**(3), 967–976 (2017).
32. I.-L. Bundalo, K. Nielsen, C. Markos, and O. Bang, "Bragg grating writing in PMMA microstructured polymer optical fibers in less than 7 minutes," Opt. Express **22**(5), 5270–5276 (2014).
33. M. C. J. Large, L. Poladian, G. W. Barton, and M. A. van Eijkelenborg, *Microstructured Polymer Optical Fibres* (Springer, 2008).
34. A. Stefani, K. Nielsen, H. K. Rasmussen, and O. Bang, "Cleaving of TOPAS and PMMA microstructured polymer optical fibers: Core-shift and statistical quality optimization," Opt. Commun. **285**(7), 1825–1833 (2012).
35. W. Yuan, A. Stefani, M. Bache, T. Jacobsen, B. Rose, N. Herholdt-Rasmussen, F. K. Nielsen, S. Andresen, O. B. Sørensen, K. S. Hansen, and O. Bang, "Improved thermal and strain performance of annealed polymer optical fiber Bragg gratings," Opt. Commun. **284**(1), 176–182 (2011).
36. N. Zhong, Q. Liao, X. Zhu, M. Zhao, Y. Huang, and R. Chen, "Temperature-independent polymer optical fiber evanescent wave sensor," Sci. Rep. **5**(1), 11508 (2015).
37. N. Zhong, M. Zhao, Q. Liao, X. Zhu, Y. Li, and Z. Xiong, "Effect of heat treatments on the performance of polymer optical fiber sensor," Opt. Express **24**(12), 13394–13409 (2016).
38. P. Stajanca, O. Cetinkaya, M. Schukar, P. Mergo, D. J. Webb, and K. Krebber, "Molecular alignment relaxation in polymer optical fibers for sensing applications," Opt. Fiber Technol. **28**, 11–17 (2016).
39. A. Pospori, C. A. F. Marques, D. Sáez-Rodríguez, K. Nielsen, O. Bang, and D. J. Webb, "Thermal and chemical treatment of polymer optical fiber Bragg grating sensors for enhanced mechanical sensitivity," Opt. Fiber Technol. **36**, 68–74 (2017).
40. A. Fasano, G. Woyessa, J. Janting, H. K. Rasmussen, and O. Bang, "Solution-Mediated Annealing of Polymer

Optical Materials EXPRESS

Optical Fiber Bragg Gratings at Room Temperature," IEEE Photonics Technol. Lett. **29**(8), 687–690 (2017).
41. C. A. F. Marques, A. Pospori, G. Demirci, O. Çetinkaya, B. Gawdzik, P. Antunes, O. Bang, P. Mergo, P. André, and D. J. Webb, "Fast bragg grating inscription in PMMA polymer optical fibres: Impact of thermal pre-treatment of preforms," Sensors (Basel) **17**(4), 1–8 (2017).
42. G. Woyessa, A. Fasano, C. Markos, H. Rasmussen, and O. Bang, "Low loss polycarbonate polymer optical fiber for high temperature FBG humidity sensing," IEEE Photonics Technol. Lett. **29**(7), 575 (2017).
43. K. Bhowmik, G.-D. Peng, Y. Luo, E. Ambikairajah, V. Lovric, W. R. Walsh, and G. Rajan, "Etching Process Related Changes and Effects on Solid-Core Single-Mode Polymer Optical Fiber Grating," IEEE Photonics J. **8**(1), 1–9 (2016).
44. E. Riande, R. Diaz-Calleja, M. Prolongo, R. Masegosa, and C. Salom, *Polymer Viscoelasticity : Stress and Strain in Practice.* (Marcel Dekker, 2000).
45. R. J. Gaymans, M. J. J. Hamberg, and J. P. F. Inberg, "Brittle-ductile transition temperature of polycarbonate as a function of test speed," Polym. Eng. Sci. **40**(1), 256–262 (2000).
46. K. Menard, *Dynamic Mechanical Analysis: A Practical Introduction* (CRC Press, 1999).
47. F. P. Incropera and D. P. DeWitt, *Fundaments of Heat and Mass Transfer* (J. Wiley, 2011).
48. A. G. Leal-Junior, A. Frizera, and M. J. Pontes, "Dynamic Compensation Technique for POF Curvature Sensors," J. Lightwave Technol. **8724**, 1–7 (2017).
49. R. Lakes, *Viscoelastic Materials* (Cambridge University Press, 2009).
50. G. Woyessa, J. K. M. Pedersen, A. Fasano, K. Nielsen, C. Markos, H. K. Rasmussen, and O. Bang, "Zeonex-PMMA microstructured polymer optical FBGs for simultaneous humidity and temperature sensing," Opt. Lett. **42**(6), 1161–1164 (2017).

1. Introduction

Optical fibers present the advantages of compactness, lightweight, multiplexing capabilities, electrical insulation and electromagnetic field immunity [1,2]. Regarding the material classification, there are two major types of optical fibers: silica and polymer optical fibers (POFs). Although they commonly present higher transmission losses [3], POFs present advantages over silica fibers such as higher fracture toughness, flexibility in bending, lower Young Modulus, higher failure strain and biocompatibility [4]. Nevertheless, it is worth to mention that some effort has been made to reduce these transmission losses through graded-index POFs [3] and their doping with different materials [5]. Because of these advantages, POF sensors have been applied to measure parameters like temperature [6], humidity [7], strain [8], refractive index [9], liquid level [10], acceleration [11]. In addition, POF sensors are employed in biomedical applications for glucose [12] and antibody detection [13,14].

To date, polymethyl methacrylate (PMMA) is the most employed material for POFs, which presents high water absorption [15]. Although such feature is advantageous in the development of humidity [16] and moisture [17] sensing applications, PMMA-based POF sensors present a higher humidity cross-sensitivity in strain and temperature applications [18]. In order to obtain a humidity insensitive operation, cyclic olefin copolymers (COC) such as Topas and Zeonex can be applied [19,20]. Just as Topas, Zeonex is humidity insensitive and has a glass transition temperature (T_g), which depends on the grade that is used, generally higher than T_g of PMMA [20,21]. Zeonex also presents a more optimal molecular weight and melt flow index, which ensures a more stable and controllable drawing, allowing for a more robust fabrication of microstructures in the fiber [20]. Since they present low losses in the Terahertz region, both Topas and Zeonex have been employed in these applications [22]. Polycarbonate (PC) POFs are also proposed as an interesting alternative for applications that require higher temperatures and strains [8].

Microstructured polymer optical fibers (mPOFs) present a pattern of holes throughout the fiber [2,23]. Such pattern presents a defined geometry and pitch between the holes, where the ratio between the hole diameter and pitch defines its modal operation. If the ratio between the hole diameter and pitch is lower than 0.43, the mPOF is endlessly single-mode [26], which means that the POF is single mode at all frequencies [19]. Another advantage of mPOFs is the possibility of holding gas or a biological sample in the holes for evanescent-wave sensing [14]. For these reasons, mPOFs are extensively employed in different sensing applications, especially those involving fiber Bragg gratings due to their endlessly single-mode operation [1,24,25]. In addition, the first single mode POF was proposed in 1991 by [26]. Then, after

Optical Materials EXPRESS

some years of research that is summarized in the review work by Zubia and Arrue [27], a single mode step index POF was reported in [28], which had a core made of Topas and a cladding of Zeonex for humidity insensitive and high temperatures operation.

One drawback of POFs is their viscoelastic nature, which leads to a non-constant response with stress or strain [29]. This behavior can lead to hysteresis in the response of a POF under stress or strain [30], which is also related to different relaxations periods of the fiber such as presented in long-term tests [31]. The Young Modulus variation of a PMMA mPOF with different frequencies were characterized in [29] and with creep recovery tests in [23]. Furthermore, the long-term viscoelastic response of a PMMA mPOF is presented in [31].

In order to obtain the response of different POF materials, namely PMMA, Topas, Zeonex and PC, this paper presents the dynamic mechanical analysis (DMA) of mPOFs made from the aforementioned materials. The DMA is also carried out on a step-index single mode POF with a Topas core and Zeonex cladding, as the one presented in [28]. The DMA involves the application of an oscillatory load with a predefined frequency and strain on the polymer samples. The tests presented in this work are made with different strains, frequencies, temperatures and relative humidity to obtain a broader understanding of the Young Modulus variation of each POF with respect to these parameters.

2. Experimental setup

The mPOFs with hexagonal patterns of holes employed in the DMA are 3-ring PC mPOF [8], 3-ring PMMA [32], 3-ring Topas grade 5013 [21] and 3-ring Zeonex 480R mPOFs [20]. In addition, a single mode step index POF with core made of Topas grade 5013 and Zeonex grade 480R cladding [28] is also employed and will be referred from now on as Topas-Zeonex step index POF. The microscope images of the cross-sectional view of each POF are presented in Fig. 1, where Fig. 1(a) presents the PMMA mPOF, whereas PC, Topas and Zeonex are presented in Fig. 1(b), (c) and (d), respectively. Also, the Topas-Zeonex step index POF is presented in Fig. 1(e). The length of the samples is about 10 mm.

The employed POFs were fabricated using the drill and draw technique, where commercial materials are casted into rods and the air-hole pattern is drilled prior to the fiber drawing [33]. Regarding the materials, they are commercial Zeonex 480R (Zeon Corporation, Japan), Makrolon LED2245 (Bayer Material Science AG, Germany) for the PC fiber, commercially available PMMA (Nordisk Plast A/S, Denmark), Topas COC grade 5013 (Topas Advanced Polymer Inc., USA). In addition, for the Topas-Zeonex step index, a single hole was made in the center of the Zeonex 480R rod and a Topas 5013S-04 was injected into the hole through an injection molding machine prior to the fiber drawing. The dimensions and geometrical parameters of each POF analyzed are presented in Table 1, which are type (mPOF or step index), cladding structure, hole diameter, pitch and core/cladding diameter.

The air holes of mPOFs reduce the homogeneity of the fiber cross sectional area that may have influence on the stress-strain cycles. In addition, such holes patterns can provide temperature insulation that may affect the temperature tests. Since the pattern of the cladding structure can lead to differences on the mechanical response, all the fibers have similar cladding structure to provide a better comparison between the materials.

Optical Materials EXPRESS

Table 1. Geometrical parameters of the POFs employed in DMA

POFs	Type	Cladding Structure	Hole diameter/pitch (μm)	Core/Cladding Diameter (μm)
PMMA	Microstructured	3 rings hexagonal	1.5/4.2	8/125
Topas 5013	Microstructured	3 rings hexagonal	2.2/6	~10/130
Topas–Zeonex step index	Step index	-	V = 2.38 at 850 nm	4.8/150
Zeonex 480R	Microstructured	3 rings hexagonal	2.2/5.5	8.8/150
Polycarbonate	Microstructured	3 rings hexagonal	1.75/4.375	7/150

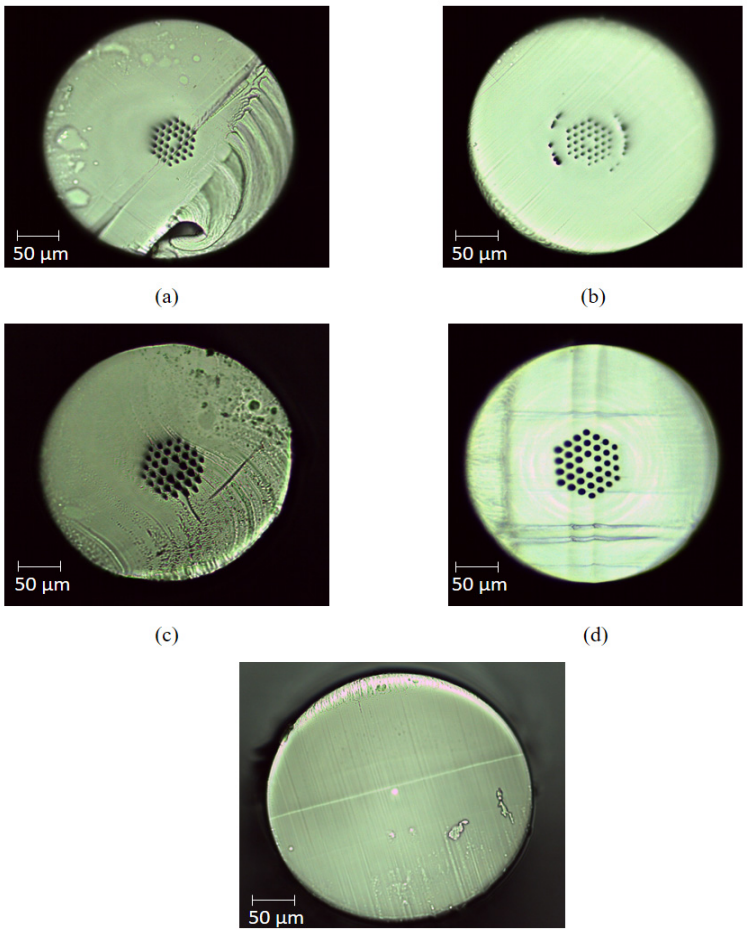

Fig. 1. Cross-sectional view of the POFs employed in this work: (a) 3-ring PMMA, (b) 3-ring PC, (c) 3-ring Topas grade 5013, (d) 3-ring Zeonex and (e) Topas-Zeonex step index.

The cleaving of mPOFs is an important process prior to its connectorization, since it can influence the quality of the mPOF surface. Therefore, the cleaving parameters such as temperature and angle need to be controlled [34]. For this reason, the employed mPOFs are

Optical Materials EXPRESS

cleaved with a hot razor blade perpendicular to the fiber, where the fiber is positioned on a plate with suitable temperatures reported for each POF material [8,20,21,32,34,35].

The effect of heat treatments on POFs was thoroughly discussed in [36,37]. The annealing is one of the heat treatments that can be made on POFs during which the fiber is kept in a temperature close, but lower than its T_g for some hours [38]. Although there are some variations of annealing, such as annealing at a controlled high humidity for better and faster annealing [7,39], application of a water/ethanol mixture to perform the annealing at room temperature [40], such process is generally made at temperatures higher than 60°C and times usually longer than 12 hours [38]. The fiber annealing can reduce the hysteresis in different sensors applications with POFs [35]. In addition, it can enhance the sensor strain sensitivity [39]. If the annealing is made on the fiber preform, it can increase the grating stability and reduce its inscription time [41], whereas, if it is made after the grating inscription, it can result in large blue-shift of the Bragg wavelength, especially when it is made under high humidity conditions [7]. Aiming at these advantages, the annealing was made in all POF samples employed. As annealing leads to a reduction of the internal stress of the POF that was created on its manufacturing process, such heat treatment has an additional advantage in the tests performed.

Since the internal stress of each POF may be different due to differences of the material drawability, it is possible that the annealing on each fiber will reduce the influence of the fiber internal stress on the material response. Table 2 presents the annealing temperature and time employed for each POF. In addition, the material T_g is also presented, since it is an important parameter to define the annealing temperature.

Table 2. The annealing parameters applied for the POFs.

POFs	Temperature (°C)	Annealing time (h)	T_g (°C)
PMMA mPOFs	80	24	110 [32]
Topas 5013 mPOFs	115	24	134 [21]
Topas–Zeonex step index	115	24	134/138 [28]
Zeonex 480R mPOF	120	24	138 [20]
Polycarbonate mPOFs	130	24	145 [8]

After the POF samples preparation with the aforementioned methods, they are positioned in the dynamic mechanical analyzer DMA 8000 (Perkin Elmer, USA) as presented in Fig. 2.

Optical Materials EXPRESS

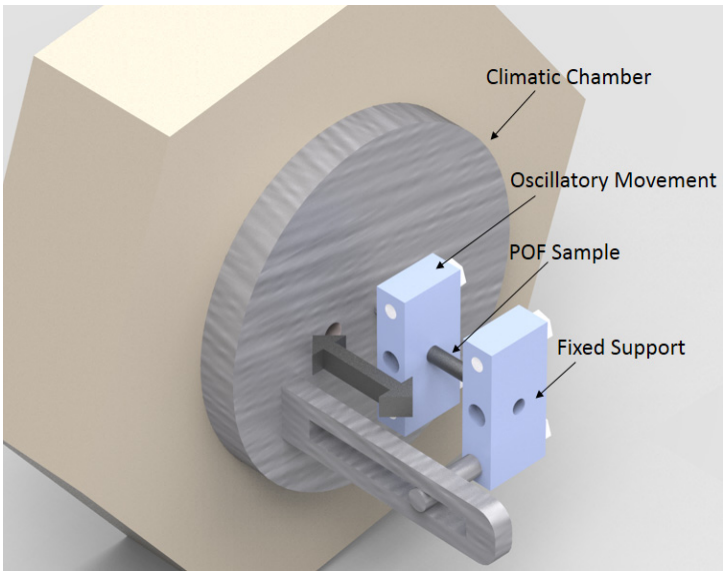

Fig. 2. Schematic view of the POF sample positioning in the DMA.

The DMA is a widely applied method to determine the mechanical properties of a viscoelastic material, by means of evaluating its Young Modulus, which has two components: elastic or storage component and the loss modulus. The dynamic Young modulus is the summation of these two components (see Eq. (1)) [30]:

$$E^* = E_0 \cos(\delta) + iE_0 \sin(\delta), \quad (1)$$

where E^* is the dynamic Young Modulus, E_0 is the static Young modulus and δ is the phase shift between the input stress or strain and the polymer response.

The Young modulus is divided into the loss and storage modulus due to the duality of a viscoelastic response, which is the combination of the elastic and viscous responses of the polymer. The loss modulus refers to the energy loss due to the viscous response, whereas the storage modulus refers to the energy storage caused by the elastic response. In order to obtain the Young Modulus of each material, stress-strain cycles are applied on each POF sample with controlled climatic conditions and frequency of the strain cycles. Then, the fibers are subjected to a constant displacement with different temperatures to obtain the Young Modulus dependency with temperature variation. Analogous tests are made with frequency and relative humidity variations in order to characterize the Young Modulus variation of each POF with these parameters.

3. Results and discussion

The strain cycle was applied on a range of 0.01% and 0.25%, where the Young Modulus is obtained by the slope of the stress-strain curves of each POF. In addition, the tests are made in a constant temperature of 25°C and relative humidity of 65%. The tests are made following the ISO 527-1:2012 standard for Young Modulus evaluation on polymers, which states that the Young Modulus of polymers is obtained by the linear regression of the stress-strain curve in a strain range of 0.05% to 0.25%. The results are presented in Fig. 3, where the linearity of each material was evaluated through the correlation coefficient (R^2). The highest linearity among the tested samples was obtained with the Topas-Zeonex step index fiber, such higher linearity is related to its higher homogeneity of the fiber cross sectional area, since this fibers do not have the air holes pattern. The same assumption explains the lower linearity obtained in the Zeonex mPOF, which is the one that presents the highest hole diameter and pitch (see

Optical Materials EXPRESS

Table 1) among the tested fibers that results in lower homogeneity of the fiber cross sectional area.

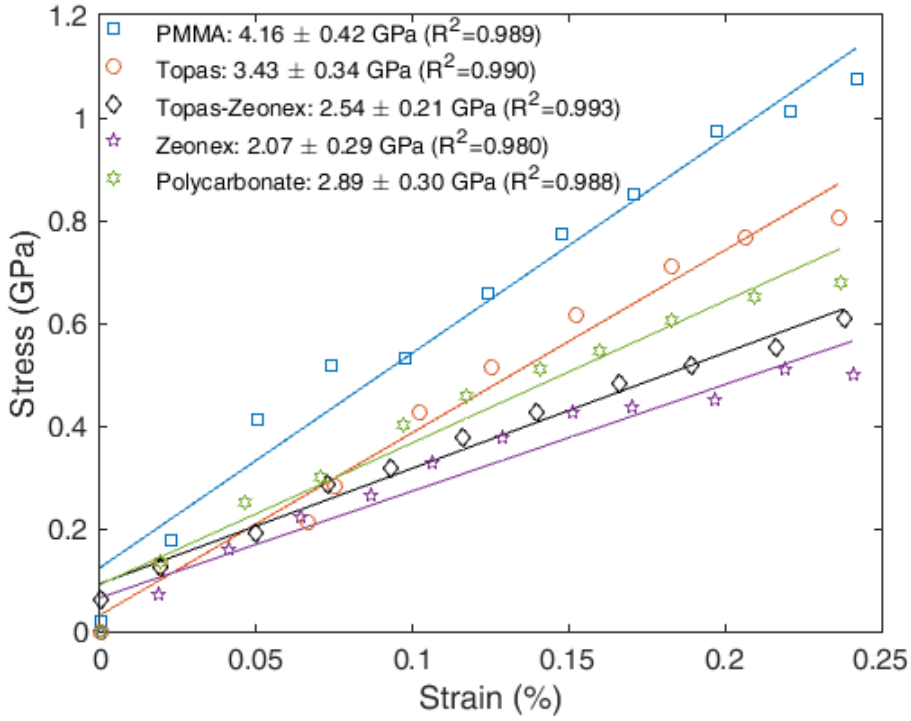

Fig. 3. Stress-strain cycles and Young's Modulus for the PMMA (blue), Topas (red), Topas-Zeonex (black), Zeonex (purple) and Polycarbonate (green) POF.

The PMMA mPOF presented the highest Young Modulus among the tested samples. In addition, the Topas and PC mPOFs presented small difference between their Young Modulus. However, as presented in [8], the PC fibers can withstand higher strains and are more suitable for large strains applications [42]. The Zeonex mPOF, on the other hand, presented the lowest Young Modulus among the evaluated materials. For this reason, such fibers may present higher sensitivity in strain sensing applications, whereas the Topas-Zeonex step index fiber presented a Young Modulus lower than the one obtained for the Topas mPOF. The reason for such difference is the Zeonex cladding that presents lower Young Modulus. Considering that the Topas-Zeonex POF presents a core diameter of 4.8 µm and a cladding of 150 µm (see Table 1), it is expected a Young Modulus value between the ones measured for the Topas and Zeonex mPOF. If there are different materials on the fiber composition, an approximation for the resulting Young Modulus can be made through Eq. (2) [43]:

$$E_{fiber} = \frac{E_c A_c + E_{cl} A_{cl}}{A_c + A_{cl}}, \tag{2}$$

where E_{fiber} is the resulting Young Modulus, E_c and E_{cl} are the Young Modulus of the core and cladding materials, respectively. Moreover, the cross-sectional areas of the core and cladding are A_c and A_{cl}, respectively. Since the Topas-Zeonex step index POF presents a cladding area higher than the core surface area, it is expected that the Young Modulus of the Topas-Zeonex POF is closer to the one of the Zeonex mPOF.

Regarding the temperature characterization, the initial temperature is about 25°C, which is the room temperature. Nevertheless, the room temperature can reach negative values such as

Optical Materials EXPRESS

−10°C or even lower in some places and the negative temperatures can lead to the ductile-brittle transition of the polymers, where the polymer starts to exhibit brittle behavior [44]. However, such transition depends on the morphology and the chain structure of the polymer. For this reason, polymers with flexible backbone usually presents ductile-brittle transitions in temperatures lower than −10°C, as an example, the transition temperature of the PC can be as low as −100°C in certain conditions [45]. Therefore, it is expected similar behavior of the Young Modulus variation in negative temperatures like −20°C, since in this temperature the ductile-brittle transition is not reached. Then, the temperature is increased at a rate of about 2°C/min until the final temperature is reached, such temperature is 100°C for the PMMA fiber due to its lower T_g and 120°C for the other POF materials, whereas the relative humidity remains constant at 65%. Figure 4 presents the Young Modulus variation of each POF with respect to the temperature.

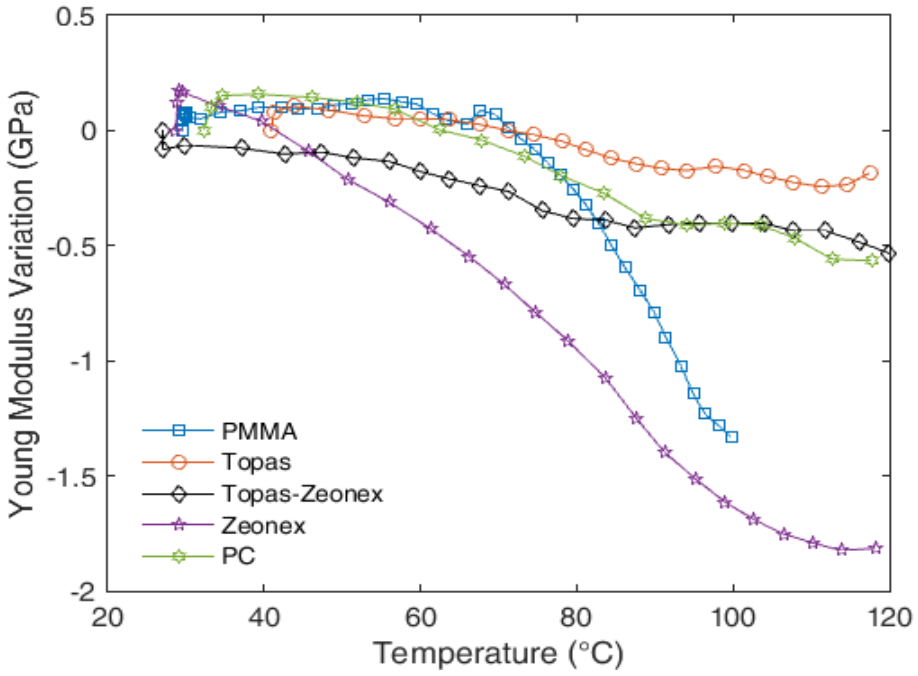

Fig. 4. Young Modulus variation with the temperature increase for the different POF materials tested.

The temperature increase leads to a molecular alignment relaxation, which causes a reduction of the material Young Modulus [38,46]. The results show a higher variation of the Zeonex mPOF with the temperature, which indicates a higher temperature cross-sensitivity that may be a disadvantage at applications with the variation of both strain and temperature. The same happens with the PMMA mPOF, which presents a lower temperature variation than the Zeonex mPOF, but it still is a high variation of about 3 times higher than the Topas-Zeonex, PC and Topas fibers when the temperature is about 100°C, where the lower temperature variation was obtained for the fibers with Topas in their composition. Although the Young Modulus of the Topas-Zeonex fiber is close to the one of the Zeonex due to the material composition discussed above and modelled in Eq. (2), the behavior of the Topas-Zeonex fiber with temperature variation is closer to the one of the Topas fiber. The reason for this behavior is related to the concept of thermal resistance, which is a parameter related to the heat conduction on each fiber. If the fiber is composed by different materials, the total

Optical Materials EXPRESS

thermal resistance (R_T) is approximated in Eq. (3) as the sum of the thermal resistance of thin elements [47].

$$R_T = \frac{r_c}{A_c + k_c} + \frac{r_{cl}}{A_{cl} + k_{cl}}, \tag{3}$$

where, r_{cl} and r_c are the radii of the core and cladding, respectively. k_c and k_{cl} are the thermal conduction coefficients of the core and cladding, respectively. Regarding the first and second terms of the sum, the first is related to the Topas and the second to Zeonex. Substituting the core and cladding geometrical parameters (see Table 1), the influence of the Topas thermal conduction is higher than the one of the Zeonex. Therefore, the thermal resistance of the Topas-Zeonex fiber is closer to the one of the Topas, which can lead to closer temperature response between Topas and Topas-Zeonex POFs. It is worth to mention that the differences between Topas and Topas-Zeonex may be related to the air-holes pattern that the Topas-Zeonex POF does not have.

In order to obtain the frequency dependency of the POF Young Modulus, tests were made with constant temperature, displacement and humidity for each POF material analyzed. The strain cycles are applied with different frequencies for each sample and the Young Modulus variation is acquired with respect to the frequency. The employed frequency range is between 0.01 Hz and 10 Hz due to operational limitations with constant temperature and relative humidity of 25°C and 65%, respectively. Nevertheless, such interval covers the frequency range for some applications, such as human movement analysis [48]. The results obtained are presented in Fig. 5, where it can be seen that all POFs analyzed presented similar behavior with slight differences between them.

The reason for the Young Modulus increase with frequency is related to the compromise between elastic and viscous behavior of a viscoelastic material, where there is a domination of a viscous-like behavior in lower frequencies [46]. As the frequency increases, the polymer tends align its molecular chains that leads to an elastic-like behavior, which is followed by the increase of the Young Modulus [46]. However, there is a region where there is an increase of the molecular movement and reduction of the Young Modulus in mPOFs [29]. Such reduction occurs between 5 Hz and 10 Hz, which is related to a constant modulus region on Young Modulus variation with respect to the frequency curve as presented in [46]. In higher frequencies is possible to observe that frequency and temperature curves present similar behavior, but in opposite directions, i.e. the Young Modulus increases with frequency and decreases with temperature [49]. Therefore, in tests with higher frequencies, the Young Modulus will increase again in frequencies higher than 10 Hz [46]. The highest modulus variation was obtained in the test with the PMMA fiber, which may indicate that this fiber may also present the highest cross-sensitivity with the movement velocity on curvature sensors applications [48]. Nevertheless, Topas-Zeonex step index POF presents the lowest frequency dependency among the ones tested, which may be advantageous in strain sensing applications where the strain presents dynamic behavior.

Optical Materials EXPRESS

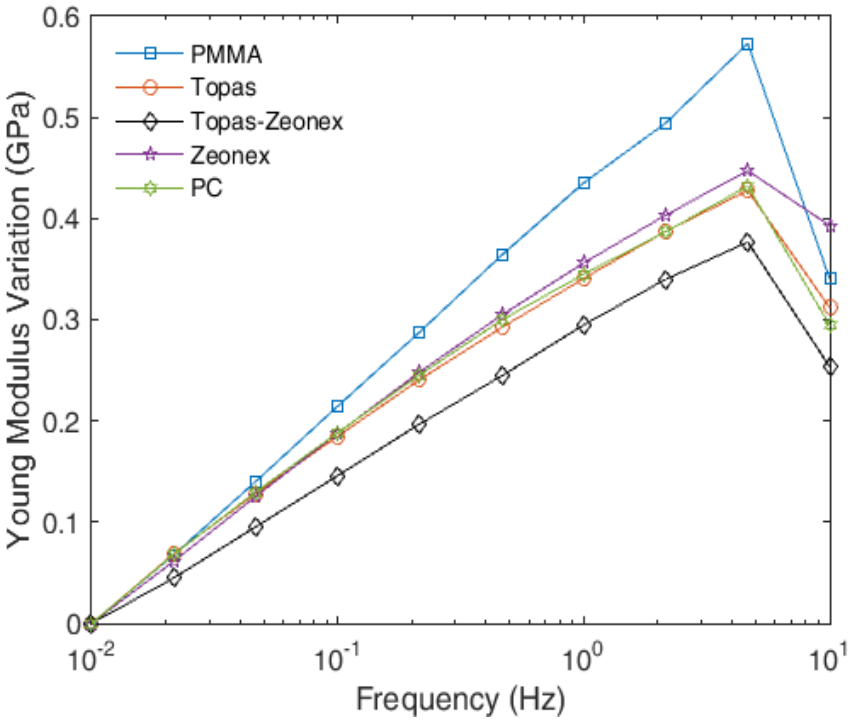

Fig. 5. Young Modulus variation in the frequency interval of 0.01 Hz to 10 Hz for different POF materials.

The last set of tests made with the POF samples is the humidity tests. These tests present some operational limitations, since the humidity needs to be kept constant for some minutes in order to enable the polymer moisture absorption. The relative humidity range of the test is from about 75% to 95%, where the lower bound of the test is maintained constant for about 30 minutes to enable the polymer water absorption. Figure 6 presents the Young Modulus variation of each POF with respect to the relative humidity for a constant relative humidity of 65%.

Regarding the humidity sensitivity, the PMMA mPOF presented the highest sensitivity among the materials tested with a Young Modulus variation three times higher than the one of the PC POF, whereas the lowest Young Modulus variation was found for the Topas mPOF and Topas-Zeonex step index POF. In particular, the modulus variation of the Topas mPOF and Topas-Zeonex step index POF was below 0.05 GPa, which makes these fibers suitable for humidity insensitive operation [19–21,28]. Therefore, the characterization of the POF materials presented here provides guidelines for the material choice for each sensor application, where some tradeoffs are to be considered when temperature, humidity, frequency and strain dependencies are accounted for. In addition, the results presented can also enable the combination of different POF materials for specific applications or conditions such as the one presented in [50].

Optical Materials EXPRESS

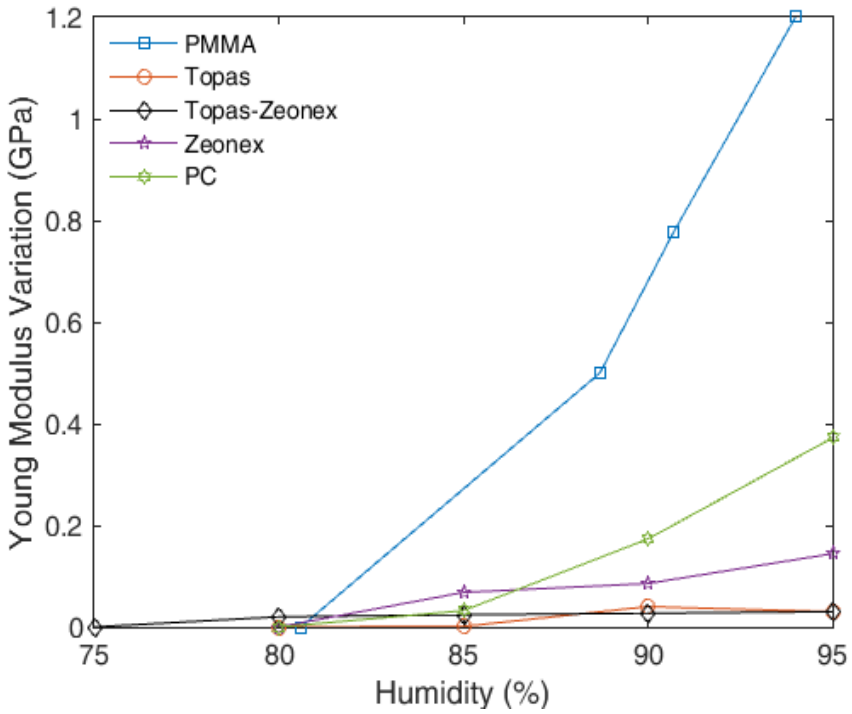

Fig. 6. Young Modulus variation with respect to the humidity variation for the different POF samples analyzed.

4. Conclusions

This paper presented the DMA in different POF materials. The POFs are annealed and positioned on a DMA equipment. First, stress-strain cycles were made on the samples in order to measure its Young Modulus, where the Zeonex mPOF shows a lower value than the other POFs, which makes it an interesting alternative when higher strain sensitivity is required. Then, temperature tests on each fiber were performed and the temperature sensitivity of each fiber was characterized with respect to their modulus variation, which show the lower Young Modulus variation with the temperature increase of Topas fibers. Additionally, Topas mPOF and Topas-Zeonex step index POF also show the lowest humidity sensitivity among the materials tested. Regarding the frequency tests, the PMMA POF presented the highest variation of Young Modulus with the frequency increase, whereas the Topas-Zeonex step index POF showed the lowest.

The results presented in this paper not only can be applied as guidelines for the material choice for a certain FBG sensor application, but also in any optical fiber sensor, since the results are obtained with respect to the intrinsic variations of the materials properties. In addition, this analysis can pave the way for applications where different materials are combined in order to obtain a specific characteristic or functionality for any sensor or optical system that relies on the POF material mechanical behavior.

Funding

CAPES (88887.095626/2015-01); FAPES (72982608); CNPq (304192/2016-3, 310310/2015-6); FCT (SFRH/BPD/109458/2015, UID/EEA/50008/2013).

Acknowledgements

The authors would like to thank the LabPetro and LabPol for the use of their DMA equipment.